1-1-2012

High contrast tandem organic light emitting devices

Baofu Ding

Xiao-Yuan Hou

Kamal Alameh
Edith Cowan University

10.1063/1.4755784

High contrast tandem organic light emitting devices

Bao-Fu Ding,[1 a)] Xiao-Yuan Hou,[2,b)] and Kamal Alameh[1,c)]
[1]*Electron Science Research Institute, Edith Cowan University, 270 Joondalup Drive, Joondalup, WA, 6027 Australia*
[2]*State Key Laboratory of Surface Physics and Key Laboratory of Micro and Nano Photonic Structures (Ministry of Education), Fudan University, Shanghai 200433, China*

A high contrast-ratio organic light emitting device (OLED) is proposed and experimentally demonstrated. The OLED is implemented by stacking two organic phase tuning layers between composite metal layers and optimizing their thicknesses. Such a tandem device can increase the current efficiency by 98%, and reduce the operating voltage by 1.04 V, in comparison to conventional high contrast OLEDs. Measured reflection spectra validate the high-contrast capability of the OLED, and demonstrate experimentally an average reflectivity of 6% under ambient light illumination. This is the lowest reflectivity reported to date for OLEDs employing organic phase tuning layers. © 2012 American Institute of Physics. [http://dx.doi.org/XXXX/XXXX]

Organic semiconductors offer several advantages, namely, variety of materials, simple fabrication processes, cost-effectiveness and transparency, which make organic optoelectronic devices attractive for many applications.[1-5] Organic light emitting diodes (OLEDs) have particularly been used in flat panel displays (FPDs) due to their wide viewing angle, ultra thin thickness requirements, low power consumption and ability to emit light without the need for external backlight sources, in addition to the possibility of growing them on flexible substrates.

In a conventional single-cell OLED, the reflective metal layer of the cathode enables the back emission from organic layer to be reflected forward resulting in a high light coupling efficiency. However, such OLEDs have the drawback of low contrast ratio due to the reflection of ambient light by the highly reflective cathode, which degrades the performance of OLEDs especially in outdoor applications where strong ambient light might be present.[2] Recently, a black composite layer has been introduced to OLED structures in order to increase the contrast ratio. This composite layer consists of a thin semi-transparent metal layer, a phase-tuning (PT) layer made of organic materials and a thick reflective metal layer,[6-8] and its low reflection is produced by the cancellation (destructive interference) of the two light waves reflected off the front thin metal layer and the rear thick metal layer which induces a π phase difference with respect to the front layer.[8] Due to their simple thermal evaporation, organic materials are considered as the best candidates for the realization of PT layers, such as tris8-hydroxyquinoline aluminum (Alq_3) (Refs. 8, 9) and copper phthalocyanineand (Ref. 10). To obtain a π phase difference, the thickness of the organic PT layer must be around 80 nm, and this is the same order of the emissive organic layer thickness. However, with a high resistance and a high carrier injection barrier between the PT layer and the intermediate metal layer, the operating voltage more than doubles, whereas, the current efficiency is reduced by 50%, because the black cathode absorbs half of the generated light from the emissive layer. The twofold increase in the operating voltage and the 50% reduction in the current efficiency reduce the overall power efficiency by 75%, thus making them impractical for emerging applications.

In this paper, we propose the use of an alternative black-layer cathode employing a composite semitransparent LiF/Al/Au in conjunction with stacked PT N,N′-di(naphthalene-1-yl)-N,N′- diphenylbenzidine (NPB)/Alq_3 layers to achieve much better current efficiency and even lower reflectivity of ambient light in comparison with conventional OLEDs employing LiF/Al as intermediate layers and Alq_3 as PT layers.[8-10]

The fabrication of this OLED was achieved by thermal sublimation of organic materials in an ultra-high vacuum environment onto a transparent glass substrate coated with indium tin oxide (ITO), similar to the process used before.[5, 11] Fig. 1 illustrates the structures and working principles of a single-cell OLED (Device 1), a conventional OLED (Device 2) and the proposed high contrast tandem OLED (Device 3). As shown in the Fig. 1(a), for Device 1, two organic layers are sandwiched between a transparent anode of indium tin oxide (ITO) and an almost-fully-reflective back metal layer, such as Al. Ambient light is fully reflected by the rear cathode Al. Ambient light penetrates through the glass substrate/ITO/ Organic layers, and mostly reflects off the thick Al mirror. Therefore, the output light of such OLED device results from both the external environment and internal active organic layer. As such, the contrast of the device is very low and its

a) Electronic mail: b.ding@ecu.edu.au
b) Electronic mail: xyhou@fudan.edu.cn
c) Electronic mail: k.alameh@ecu.edu.au

visual image is poorly seen as shown by the photograph in Fig. 1(a). Fig. 1(b) shows the schematic diagram of a conventional high-contrast OLED with an organic PT layer (Device 2). Compared to the structure of Device 1, there is an additional metal-organic-metal (MOM) structure on the top of the emissive cell. The LiF (<1 nm)/Al (<8 nm) were used as semitransparent intermediate layers. Ambient light penetrates through the glass substrate and the emissive layer, and partially reflects off the semitransparent intermediate layers. The transmitted light through the latter reflects off the Al mirror and interferes with the light reflected off the intermediate layers. The phase difference $\Delta\varphi$ between the two light waves reflected off the upper and lower cells is expressed as:

$$\Delta\varphi = \frac{2n(\lambda)\cdot d}{\lambda} \quad (1)$$

where n, d and λ are the refractive index, thickness of the PT layer and the wavelength of light, respectively. Factor 2 in the Eq. (1) is due to the round trip of the light wave in the PT layer. By changing d, $\Delta\varphi$ can be varied in the range of 0~π. For $\Delta\varphi=\pi$, destructive optical interference occurs as illustrated. The cancellation of the two reflected light beams results in a dark cathode as shown by the photograph in Fig. 1(b). Based on the MOM black structure illustrated in Fig. 1(b), the design of the proposed high contrast tandem OLED (Device 3) is illustrated in Fig. 1(c). It consists of an upper cell (coated with a thick Al mirror) and a lower cell connected through semi-transparent intermediate nano-layers. Compared to the structure of Device 2, bilayers of Au (7 nm)/NPB (20 nm) are inserted between the intermediate layer of Al (4 nm) and the PT layer of Alq_3. Due to the low work function of composite LiF/Al layers and the high work function of Au layer,[12] the intermediate layers of LiF/Al/Au act as the cathode for the lower cell and the anode for the upper cell, respectively. Thus LiF/Al/Au can be called an anode-cathode layer (ACL).[13] Therefore, while both upper and lower cells emit light, the PT mechanism ensures that the tandem OLED device attains high contrast operation by changing the thickness of Alq_3 layer in the upper cell.

Fig. 2(a) shows the measured brightness-current density characteristics for the three devices. It is obvious from Fig. 2(a) that the brightness of Device 2 is approximately half of that of Device 1 at a given current density. For instance, at 40 mA/cm^2, the electroluminescence (EL) of Device 2 is 2500 cd/m^2, compared with 4050 cd/m^2 EL for Device 1 at the same current density. Such reduction in luminance for Device 2 is due to the additional MOM black cathode introduced on top of the bottom emissive cell.[8] Therefore, even if the PT layer thickness is optimized to suppress the reflected light through destructive optical interference, the current efficiency of this OLED structure is limited since half of the generated light is lost by the black cathode. Therefore, the theoretical limit of current the efficiency in such black-cathode- based OLEDs is only half of that of conventional counterparts. However, for the proposed Device 3, the EL at the same current density dramatically increases to 4930 cd/m^2, and in comparison with Device 2, EL increases by 98%. Interestingly, the EL of Device 3 is even higher than that of Device 1. Our measured results show that besides the bottom cell, the top MOM structure of Device 3 contributes to photon emission as well. In the MOM structures, the interfaces between intermediate layers and the PT layers in Device 2 and Device 3 are Al/Alq_3 and Au/NPB respectively.

Generally, the hole-injection barrier ϕ_B in this interface is the energy difference between the work function of the composite intermediate layer and the highest occupied molecular orbit (HOMO), which is analogous to the top of the valence band in an inorganic semiconductor.

Fig. 2(b) illustrates the energy level diagrams of the interfaces between the composite intermediate layer and the PT layer for Device 2 and Device 3. The work function of Al and the HOMO of Alq_3 are respectively 4.3 eV and 5.7 eV,[14] ϕ_B is 1.4 eV, which is high enough to prevent hole injection from the composite intermediate layer to the PT layer, restricting the exciton formation and photon emission in the PT layer. As for Device 3, the work function of Au and HOMO of NPB are 5.1 eV and 5.4 eV, respectively.[14, 15] Thus ϕ_B is reduced from 1.4 eV for Device 2 to 0.3 eV for Device 3, and this barrier is low enough for hole injection from Au to NPB. The low hole-injection barrier enables light emission from the upper cell. Fig. 2(c) and 2(d) show the charge-to-photon processes for a single-cell based OLED and a tandem OLED, respectively. For a single cell, the OLED can emit one photon at most when an electron and a hole are injected from the external circuit into the organic emissive layer, as illustrated in Fig. 2(c). On the other hand, in a tandem OLED, the additional intermediate ACL functions as a charge generating layer, which offers, under an external applied electric field, an electron for the lower cell and a hole for the upper cell. As shown in Fig. 2(d), if the electron-injection barrier of the lower cell and the hole-injection barrier of the upper cell are low enough, the generated electron and hole in the ACL can be efficiently injected into the two cells, where they interact through Coulomb effects with the hole and the electron injected from the external circuit to form new excitons. Therefore, an injected electron and an injected hole from the external circuit can generate two excitons inside the tandem OLED, leading to a 2-fold increase in current efficiency, in comparison with a single-cell based OLED.

Noticeably, for Device 2 and Device 3, both the lower cell and the upper MOM structure contain Alq_3, making it hard to distinguish which cell dominates the light emission. To directly track the light emitting source, two different fluorescent materials in the lower cell and upper cell were employed.

Fig. 3 shows the structure of an additional OLED (Device 4). In the upper cell, namely the MOM structure, the Alq_3 layer in Device 3 was replaced by a DCM1 doped Alq_3 layer, where DCM1 is the fluorescent dye 4-(dicyanomethylene)-2-methyl-6-.(p-dimethylaminostyry l e) 4H-pyran. The doping ratio in weight was around 3%, which is high enough for quenching

all excitons in the host Alq_3 and forming excitons in DCM1 through "Förster Energy Transfer" and "Charge Trapping" from the host of Alq_3 to the dopant DCM1.[16] Thus the emissive molecules in the upper cell are DCM1 rather than Alq_3. The EL spectrum of Device 4 under a bias voltage of 12 V is also plotted in Fig. 3, displaying two different peaks around 530 nm and 610 nm, which are in good agreement with the EL spectra of Alq_3 and DCM1, respectively.[16] Therefore, both cells in Device 4 emit photons, as evident from the two-peak spectrum, implying that the composite LiF/Al/Au layer works as an efficient anode-cathode layer.

Fig. 4 shows the J-V characteristics for the three devices. At a current density of 40 mA/cm^2, the operating voltage of Device 2 is 13.2 V, almost 7 V higher than that of Device 1. This indicates that the extra 80 nm thick Alq_3 higher than that of Device 1, and that the extra 80 nm thick Alq_3 layer introduces a considerably high resistance, resulting in a remarkably higher operating voltage. This is consistent with previous reported results.[17] For Device 3, the operating voltage is 1.04 V lower than that of Device 2. Since ϕ_B of the MOM structures for both Device 2 and Device 3 is higher than 0.2 eV, the current flow through the MOM is dominated by the injection limited current (J_{ILC}) as described in Ref. 18, which is expressed as:

$$J_{ILC} = q\mu EN \exp\left(-\frac{q\phi_B}{kT}\right)\exp\left(\frac{q\gamma}{kT}\sqrt{E}\right) \quad (2)$$

where q is the electron charge, μ is the hole mobility, E is the electric field, N is the density of state, and ϕ_B is the hole injection barrier. From Eq. (2), if ϕ_B is reduced, at a given current, E will also reduce accordingly. With E being proportional to V/L , where V is the operating voltage and L is the thickness of organic layer, the reduction of ϕ_B leads to the reduction of the operating voltage.

Fig. 4(a) shows the optical reflectance spectra of Devices 1-3 measured at a 5° off the surface normal. The average reflectance of the OLED is 80% for Device 1, 20% for Device 2, mainly due to the addition of the MOM structure. Since there are two PT layers in Device 3, Eq. (1) need to be expanded as :

$$\Delta\varphi = \frac{2\left[n_1(\lambda)\cdot d_1 + n_2(\lambda)\cdot d_2\right]}{\lambda} \quad (3)$$

where $n_1(\lambda)$ and $n_2(\lambda)$ are the refractive indices of NPB and Alq_3 respectively, and d_1 and d_2 are the thicknesses, of NPB and Alq_3, respectively. To attain maximum destructive interference with the stacked NPB/Alq_3 PT layers in Device 3, the phase difference between the two light waves reflected off the upper and lower cells should be π. The spectral range of the ambient visible light extends from 400 nm to 750 nm, however, the elimination of the light around 550 nm is the main concern since 550 nm is the most sensitive wavelength to the human eyes. As shown in Fig. 4(b), at 550 nm, the refractive indices of Alq_3 and NPB are 1.7 and 1.8 respectively. With the NPB thickness being fixed at 20 nm, the optimal Alq_3 thickness is 59 nm, according to Eq. (3). The measured reflectance from the proposed Device 3 was only 6.0% over the range of 400 to 750 nm. As we know, this is the lowest reflectivity among all high contrast OLEDs based on the use of an organic PT layer. While in the human-eye-sensitive range of 500-600 nm, the reflection value is further reduced to 4%, which nearly approaches the minimum limitation value since the reflectance of air/glass is around 4%.

We have proposed and demonstrated the concept of a high contrast-ratio organic light emitting device (OLED) realized through the stacking of two organic phase tuning layers between composite metal layers. Experimental results have demonstrated an increase in current efficiency by 98%, a reduction in operating voltage by 1.04 V and an ambient reflection as low as 6%, which are respectively attributed to the photon emission from the PT layer, the reduced hole injection barrier between the intermediate layer and the PT layer, and a proper optical design.

This research is supported by Edith Cowan University, the Department of Industry, Innovation, Science, Research and Tertiary Education, Australia, and National Natural Science Foundation of China (NSFC] and Ministry of Science and Technology of China.

[1]C. W. Tang, Appl. Phys. Lett. **48**, 183 (1986).
[2]C. W. Tang and S. A. Vanslyke, Appl. Phys. Lett. **51**, 913 (1987).
[3]R. H. Friend, R. W. Gymer, A. B. Holmes, J. H. Burroughes, R. N. Marks, C. Taliani, D. D. C. Bradley, D. A. Dos Santos, J. L. Bredas, M. Logdlund and W. R. Salaneck, Nature **397**, 121 (1999).
[4]C. D. Dimitrakopoulos and P. R. L. Malenfant, Adv. Mater. **14**, 99 (2002).
[5]B. F. Ding, Y. Q. Zhan, Z. Y. Sun, X. M. Ding, X. Y. Hou, Y. Z. Wu, I. Bergenti and V. Dediu, Appl. Phys. Lett. **93**, 183307 (2008).
[6]L. S. Hung and J. Madathil, Adv. Mater. **13**, 1787 (2001).
[7]A. N. Krasnov, Appl. Phys. Lett. **80**, 3853 (2002).
[8]X. D. Feng, R. Khangura and Z. H. Lu, Appl. Phys. Lett. **85**, 497 (2004).
[9]Y. C. Zhou, L. L. Ma, J. Zhou, X. D. Gao, H. R. Wu, X. M. Ding and X. Y. Hou, Appl. Phys. Lett. **88,** 233505 (2006).
[10]J. H. Lee, C. C. Liao, P. J. Hu and Y. Chang, Synth. Met. **144**, 279 (2004).
[11]B. F. Ding, Y. Yao, Z. Y. Sun, C. Q. Wu, X. D. Gao, Z. J. Wang, X. M. Ding, W. C. H. Choy and X. Y. Hou, Appl. Phys. Lett. **97**, 163302 (2010).
[12]J. Y. Lee, Appl. Phys. Lett. **88**, 073512 (2006).
[13]V. Shrotriya, E. H.-E. Wu, G. Li, Y. Yao and Y. Yang, Appl. Phys. Lett. **88**, 064104 (2006).
[14]H. Ishii, K. Sugiyama, E. Ito and K. Seki, Adv. Mater. **11**, 605 (1999).
[15]J. Cao, X. Y. Jiang and Z. L. Zhang, Appl. Phys. Lett. **89,** 252108 (2006).
[16]B. F. Ding, Y. Yao, C. Q. Wu, X. Y. Hou and W. C. H. Choy, J. Phys. Chem. C 115, 20295 (2011)
[17]P. E. Burrows, V. Bulovic, S. R. Forrest, L. S. Sapochak, D. M. McCarty and M. E. Thompson, Appl. Phys. Lett. **65**, 2922 (1994).
[18]S. G. Lee and R. Hattori, Journal of Information Display **10**, 143 (2009).

Figure captions:

Fig. 1 Schematic diagram illustrating the design of the high contrast tandem OLED. The structures and photographs of (a) a conventional single cell OLED (Device 1), (b) the single cell OLED with a phase tuning layer (Device 2) and (c) the proposed high contrast tandem OLED (Device 3) illuminated with ambient light.

Fig. 2 (a) *B-J* characteristics of three devices, namely Device 1: single-cell OLED, Device 2: high contrast OLED with the PT layer and Device 3: proposed high contrast tandem OLED. (b)Energy diagrams for Device 2 and Device 3 at the interface between the intermediate layers and the PT layer. Charge-to-photon processes for (c) a single-cell based OLED and (d) a tandem OLED.

Fig. 3 EL spectrum of Device 4 with two different emissive materials.

Fig. 4 *J-V* characteristics of Devices 1, 2 and 3**.**

Fig. 5 (a) Reflectivity of Device 1, 2 and 3, and (b) refractive indices of NPB and Alq_3.

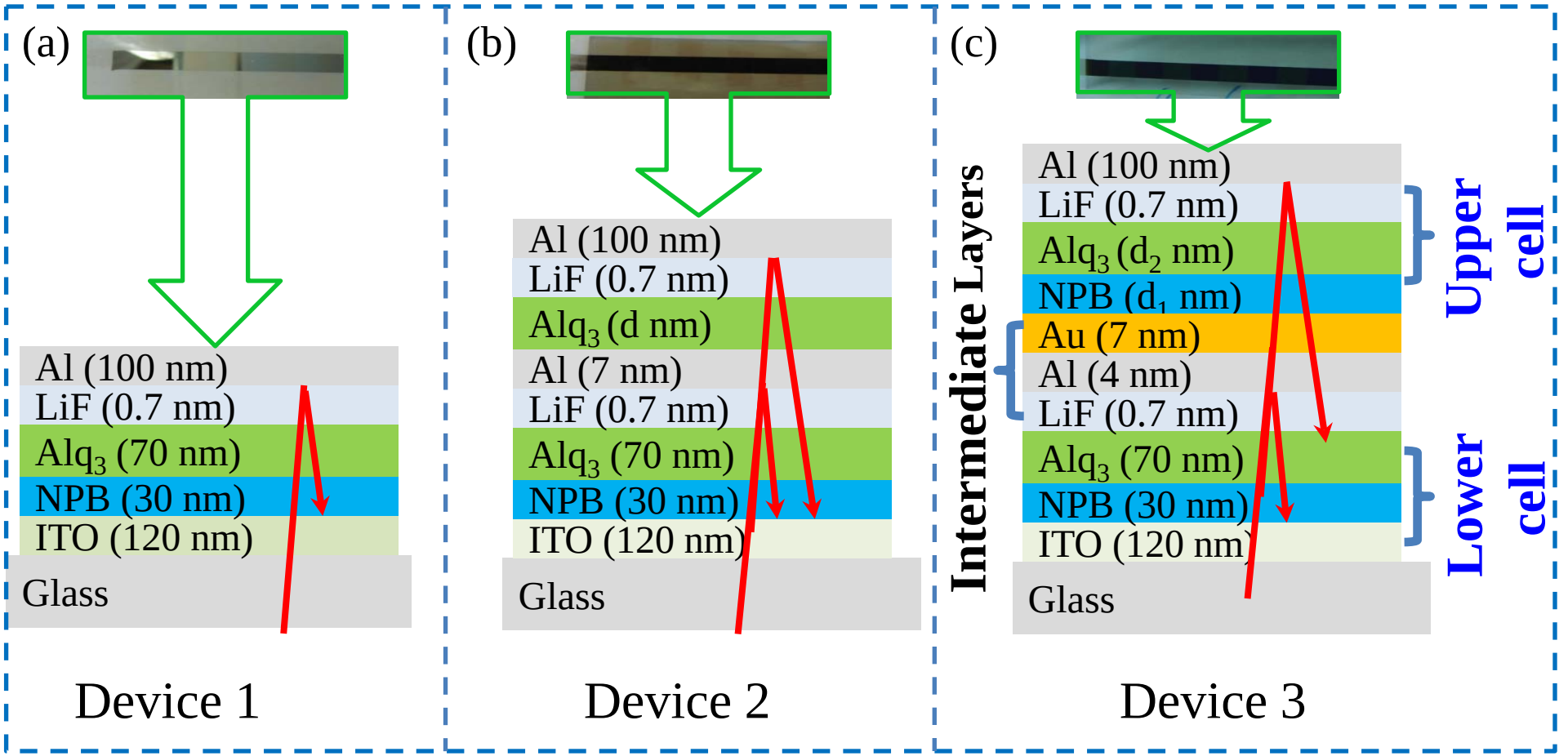
(a)
Al (100 nm)
LiF (0.7 nm)
Alq3 (70 nm)
NPB (30 nm)
ITO (120 nm)
Glass
Device 1
(b)
Al (100 nm)
LiF (0.7 nm)
Alq3 (d nm)
Al (7 nm)
LiF (0.7 nm)
Alq3 (70 nm)
NPB (30 nm)
ITO (120 nm)
Glass
Device 2
(c)
Intermediate Layers
Al (100 nm)
LiF (0.7 nm)
Alq3 (d2 nm)
NPB (d1 nm)
Au (7 nm)
Al (4 nm)
LiF (0.7 nm)
Alq3 (70 nm)
NPB (30 nm)
ITO (120 nm)
Glass
Upper cell
Lower cell
Device 3

(a)

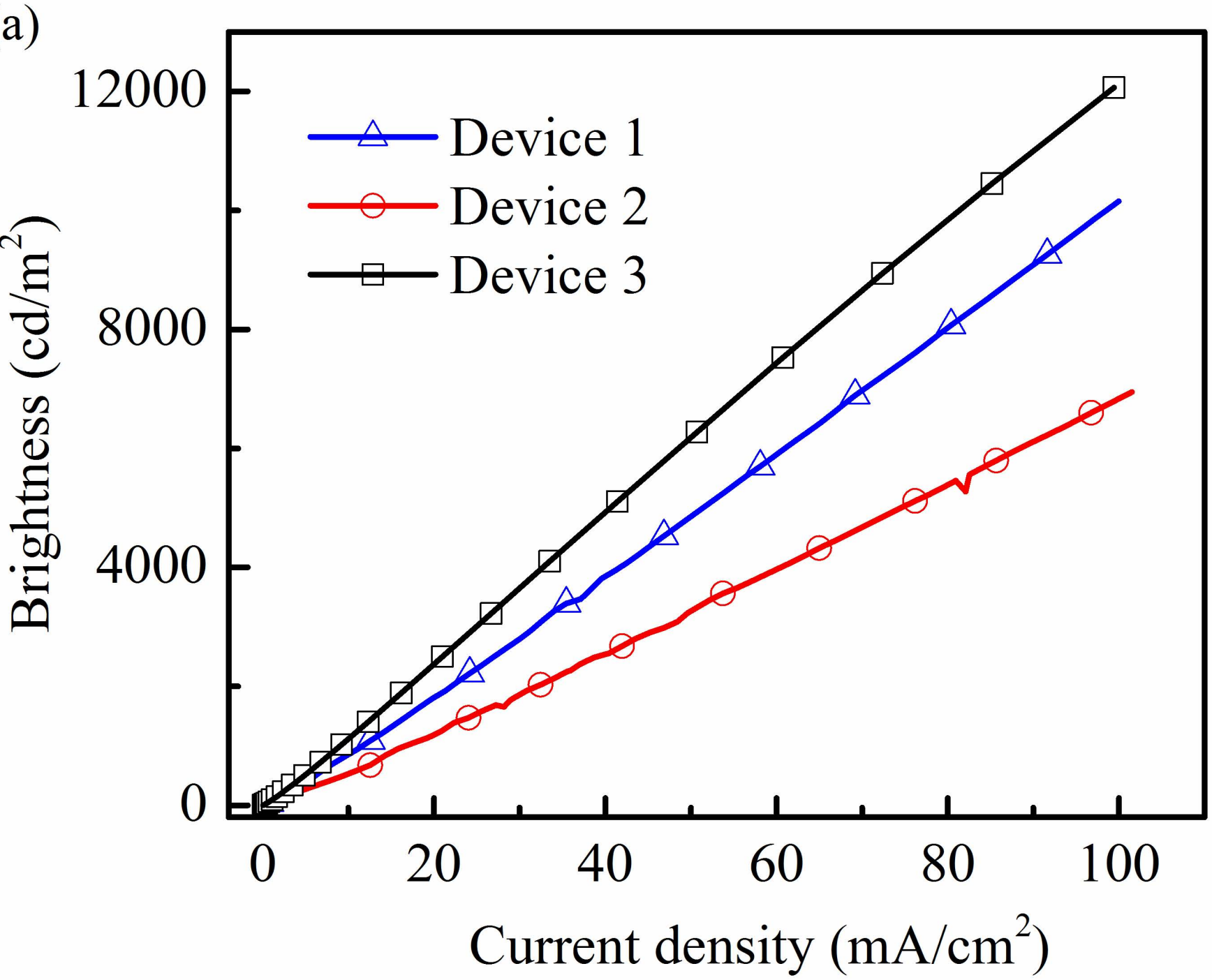
12000
8000
4000
0
Brightness (cd/m^2)
Device 1
Device 2
Device 3
0
20
40
60
80
100
Current density (mA/cm^2)

(b)

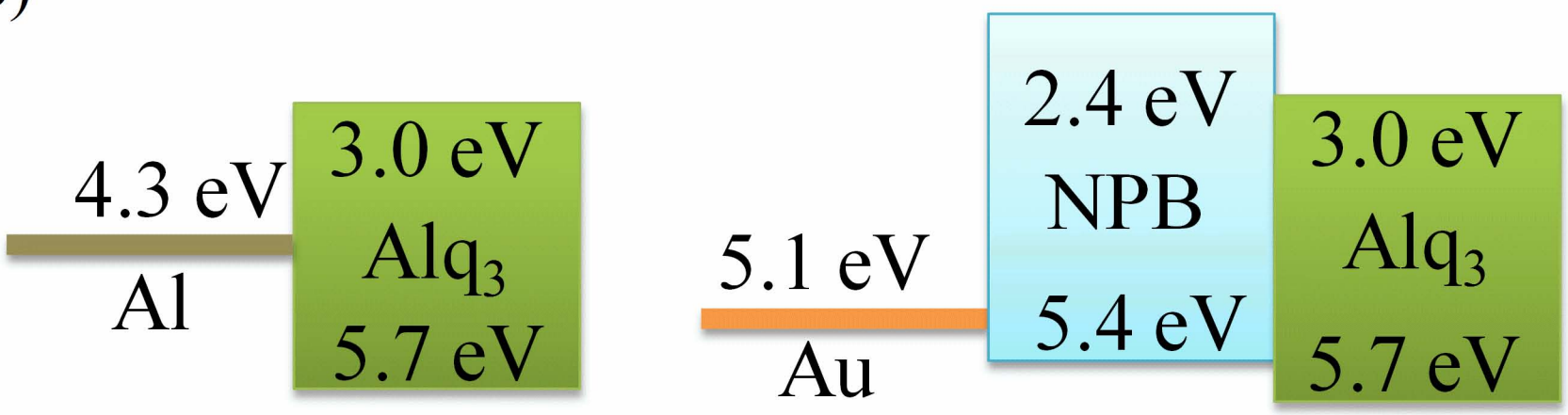
4.3 eV
Al
3.0 eV
Alq3
5.7 eV
5.1 eV
Au
2.4 eV
NPB
5.4 eV
3.0 eV
Alq3
5.7 eV

(c)

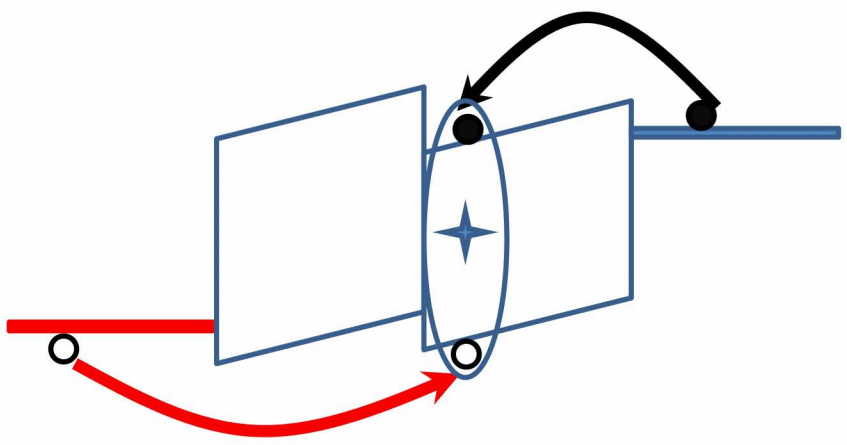

(d)

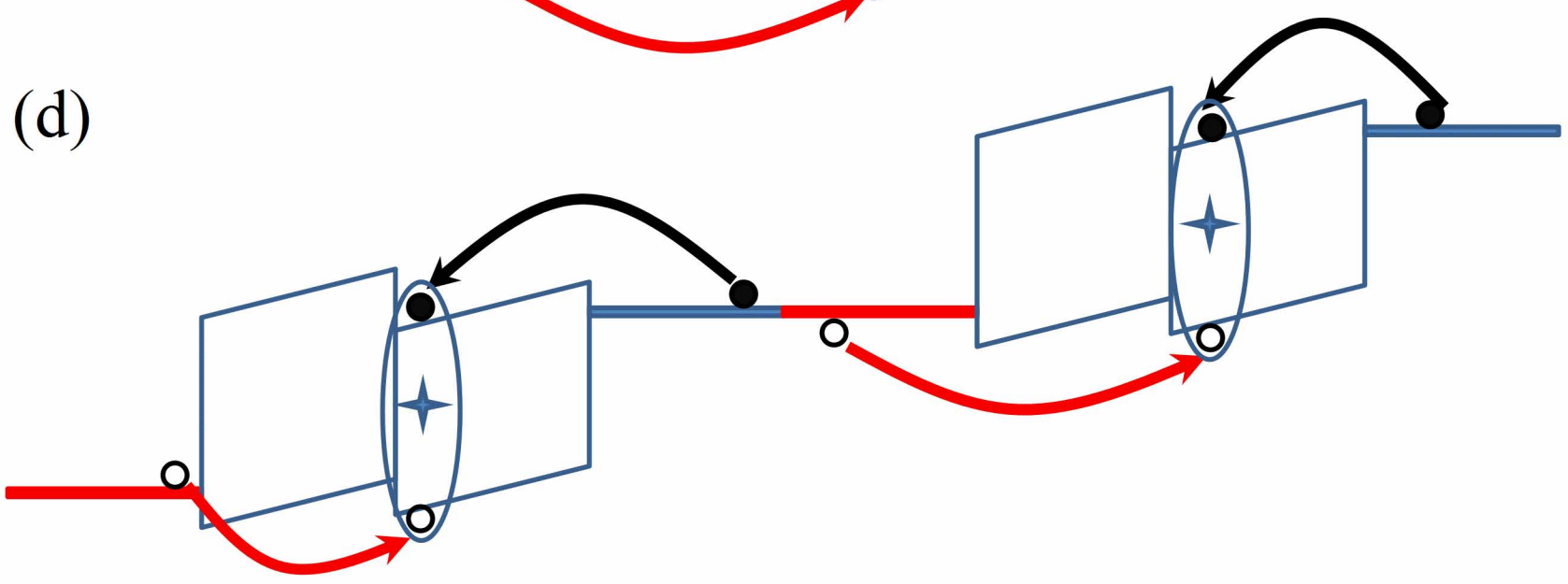

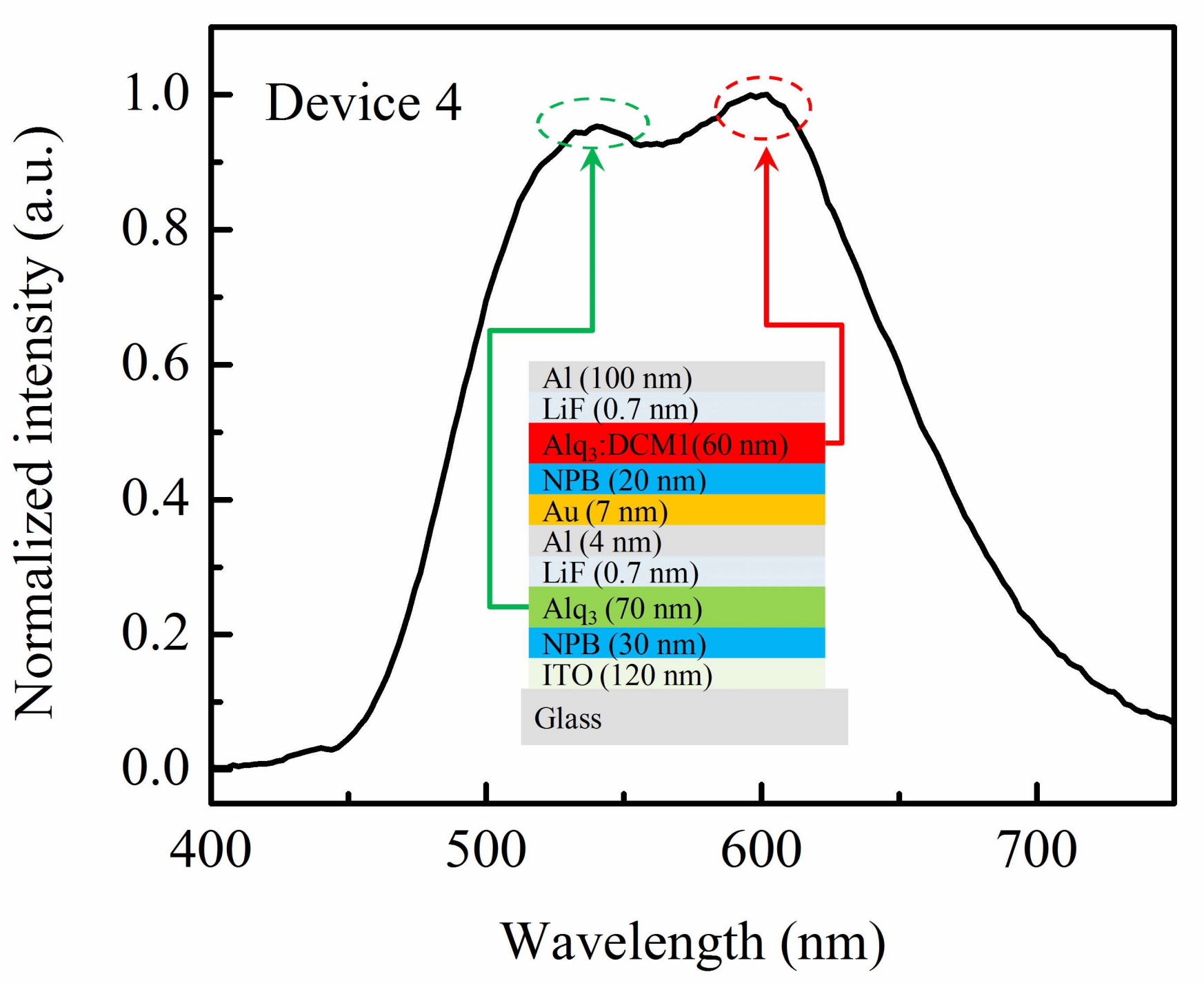
Device 4
Normalized intensity (a.u.)
1.0
0.8
0.6
0.4
0.2
0.0
400
500
600
700
Wavelength (nm)
Al (100 nm)
LiF (0.7 nm)
Alq3:DCM1(60 nm)
NPB (20 nm)
Au (7 nm)
Al (4 nm)
LiF (0.7 nm)
Alq3 (70 nm)
NPB (30 nm)
ITO (120 nm)
Glass

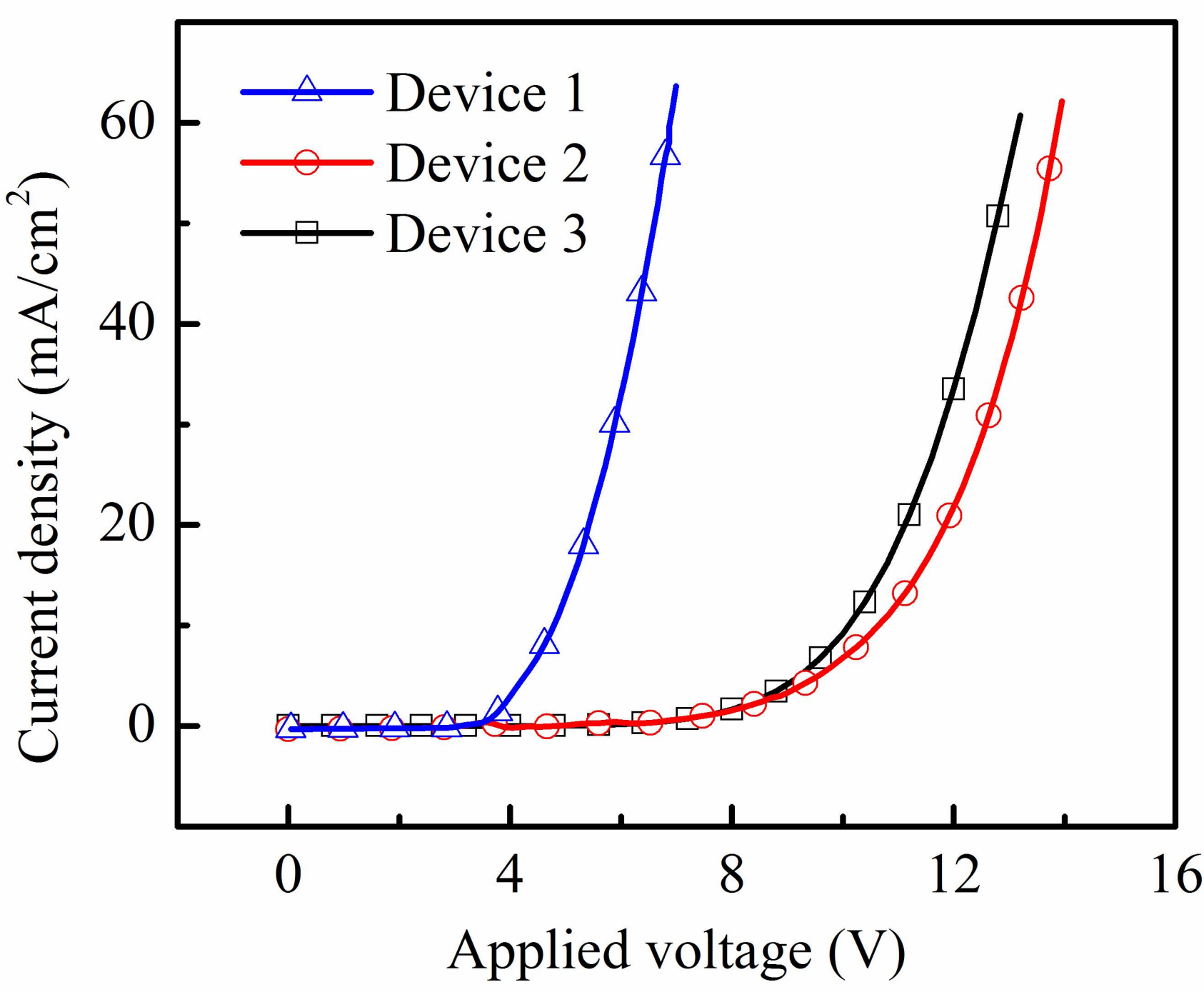
Device 1
Device 2
Device 3
Current density (mA/cm^2)
Applied voltage (V)
0
20
40
60
0
4
8
12
16

(a)

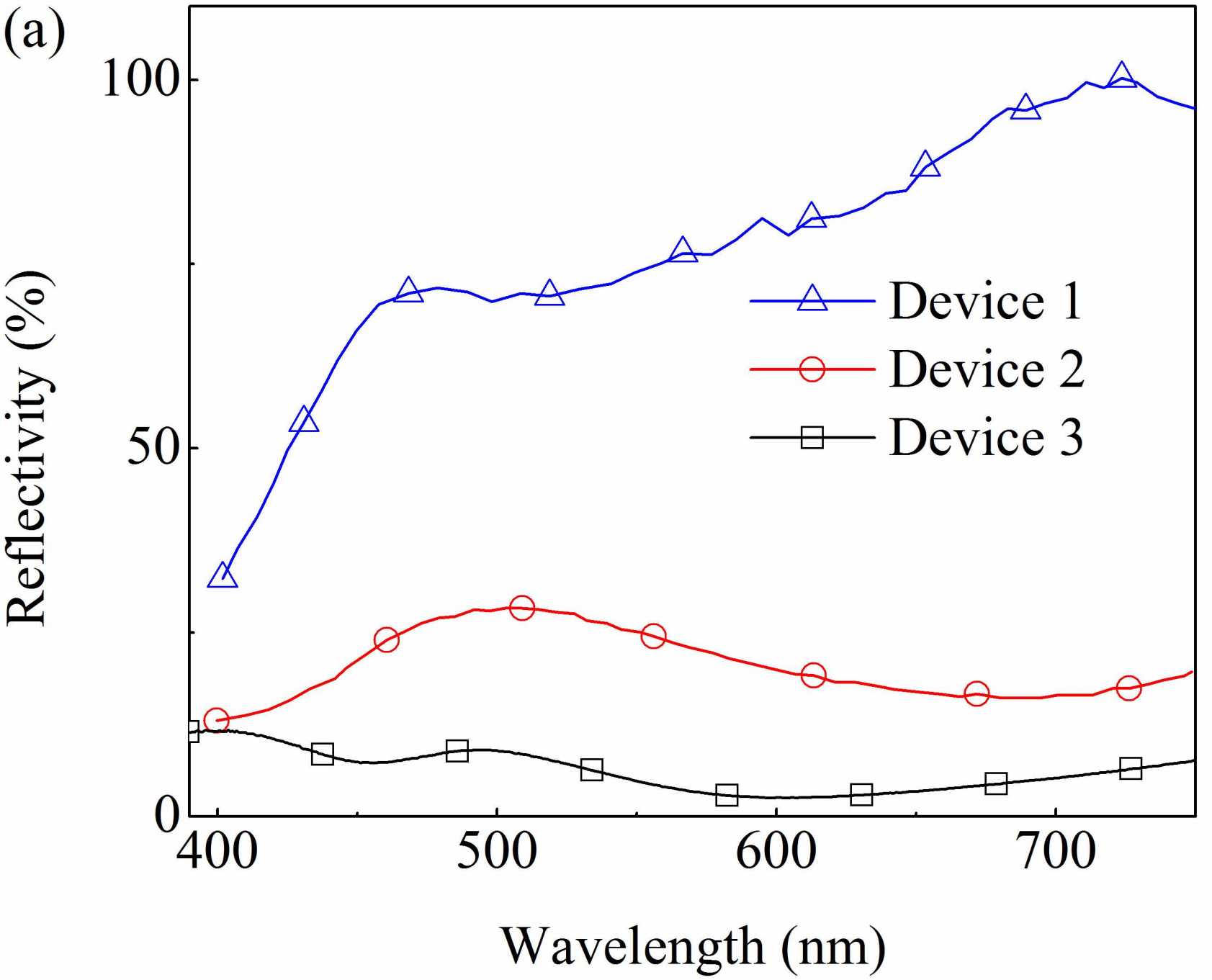
100
50
0
Reflectivity (%)
400
500
600
700
Wavelength (nm)
Device 1
Device 2
Device 3

(b)

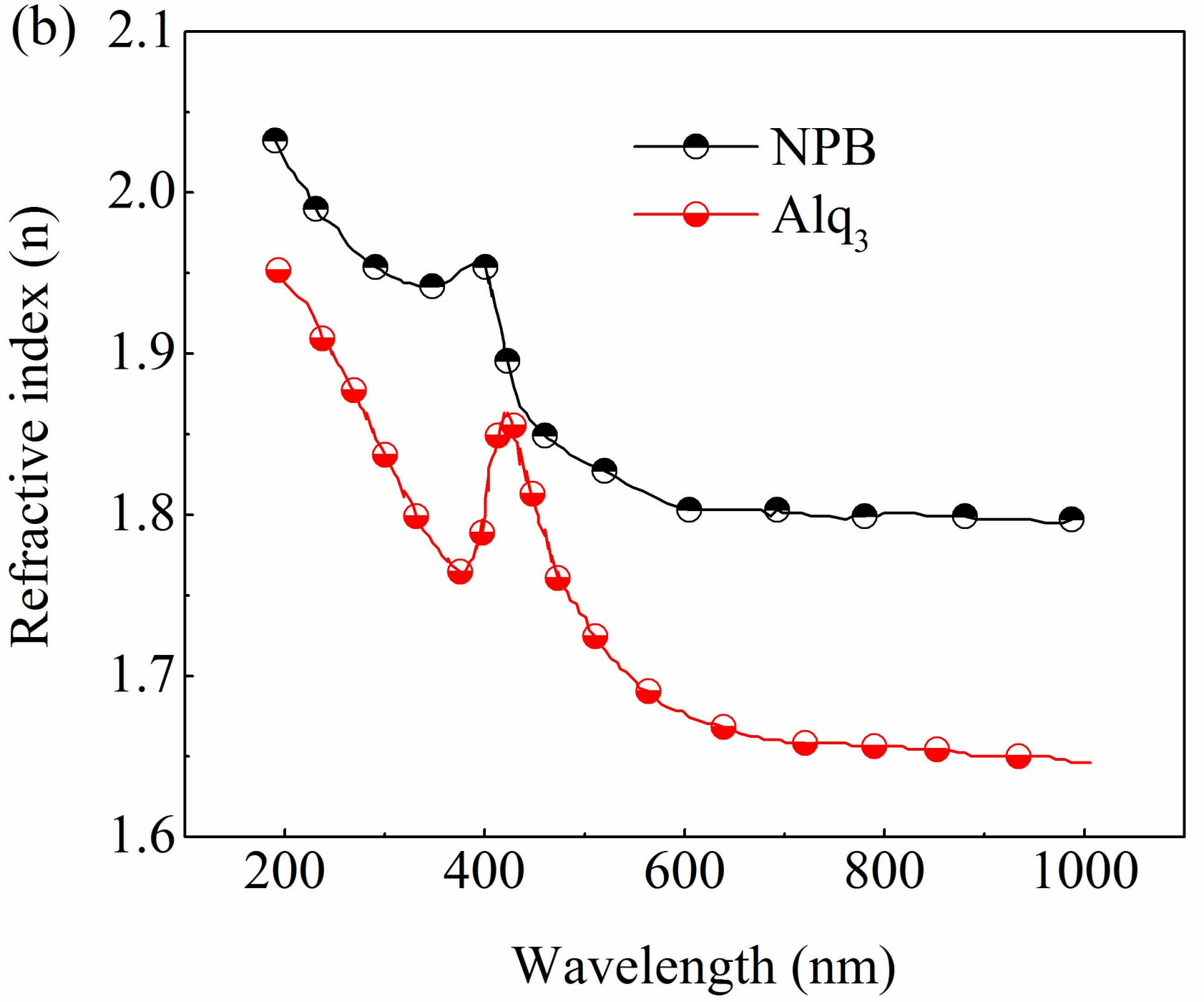
2.1
2.0
1.9
1.8
1.7
1.6
Refractive index (n)
200
400
600
800
1000
Wavelength (nm)
NPB
Alq3